

SUPPLEMENTAL INFORMATION

CDK4 is an essential insulin effector in adipocytes

Sylviane Lagarrigue, Isabel C. Lopez-Mejia, Pierre-Damien Denechaud, Xavier Escoté, Judit Castillo-Armengol, Veronica Jimenez, Carine Chavey, Albert Giralt, Qiuwen Lai, Lianjun Zhang, Laia Martinez-Carreres, Brigitte Delacuisine, Jean S. Annicotte, Emilie Blanchet, Sébastien Huré, Anna Abella, Francisco J. Tinahones, Joan Vendrell, Pierre Dubus, Fatima Bosch, C. Ronald Kahn, and Lluís Fajas

Inventory:

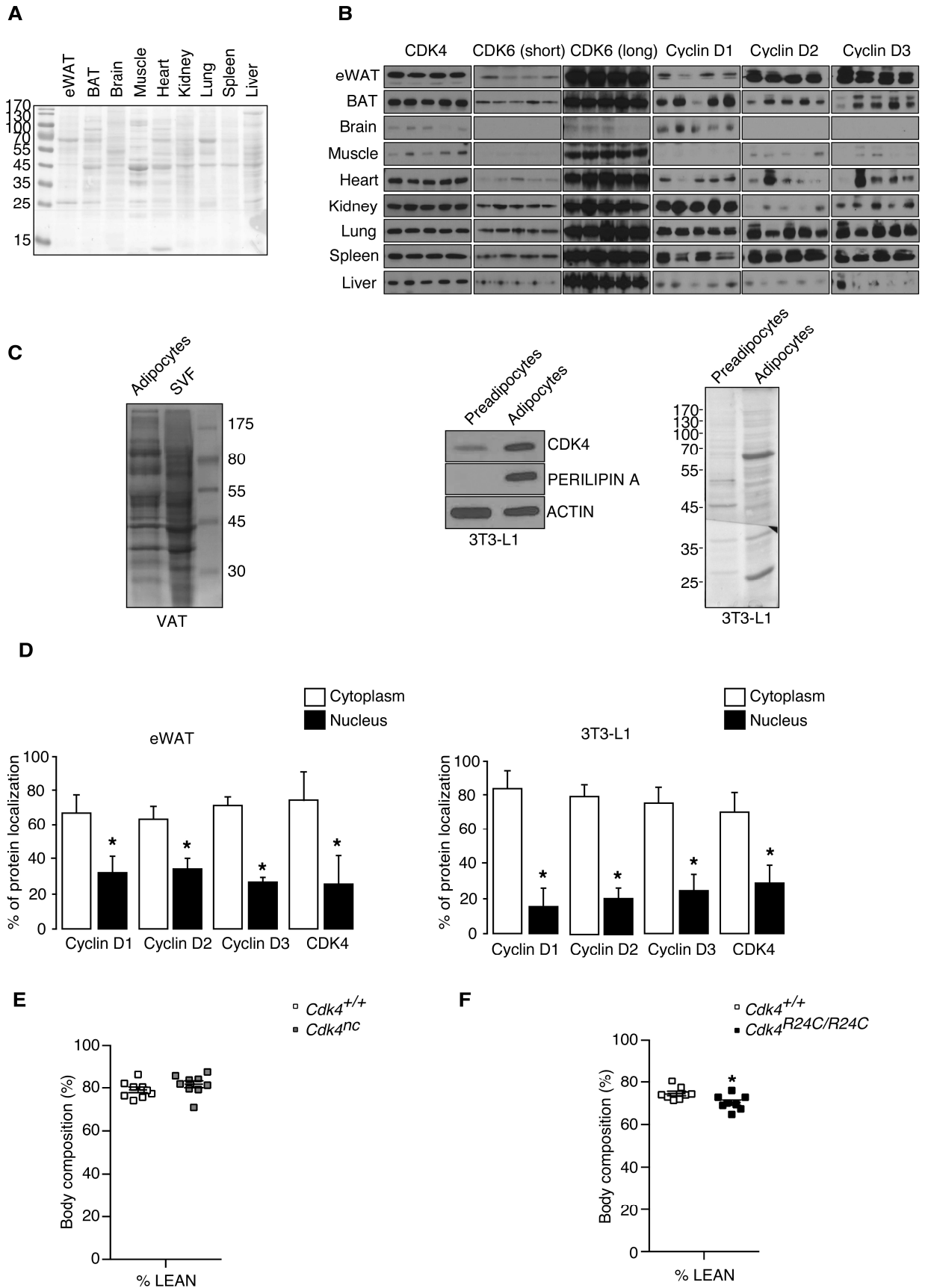
Supplemental Figure 1-6 and table 1

Supplemental Experimental Procedures

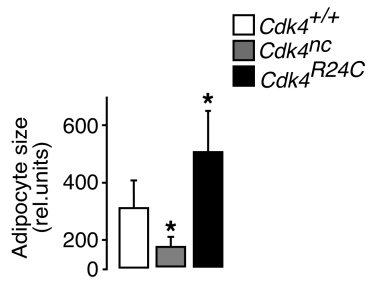
Supplemental References

SUPPLEMENTAL FIGURES 1-6 and table 1

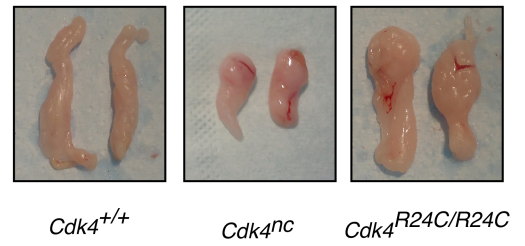
Supplemental Figure 1. (A) Ponceau staining of figure 1A. (B) Immunoblot analysis of CDK4, CDK6, Cyclin D1, Cyclin D2 and Cyclin D3 protein expression in different tissues (n=4 for eWAT and spleen and n=5 for others tissues). (C) Ponceau staining from VAT and 3T3-L1 adipocytes from VAT digestion and 3T3-L1 fractionation as indicated. CDK4 protein level in pre-adipocytes and mature adipocytes isolated from 3T3-L1. The blots for VAT is shown in figure 1B (D) Quantification of the subcellular localization of CDK4 and Cyclin D1, Cyclin D2 and Cyclin D3 proteins in cytoplasm and nuclear fractions of eWAT and mature 3T3-L1 adipocytes. The blots are shown in figure 1C. (E-F) Percentage of lean mass of 20-week-old *Cdk4^{+/+}* and *Cdk4^{nc}* mice (n= 9) (E) and 30-week-old *Cdk4^{+/+}* and *Cdk4^{R24C/R24C}* mice (n= 8) (F). (G) Adipocyte size quantification in *Cdk4^{+/+}*, *Cdk4^{nc}*, and *Cdk4^{R24C/R24C}* mice. (H) Representative images of eWAT in the indicated *Cdk4* mouse genotypes, showing atrophy and hypertrophy in 24-week-old- *Cdk4^{nc}* and *Cdk4^{R24C/R24C}* mice respectively. (I) The targeting strategy for the generation of a conditional CDK4 KO mice is schematized here. (J) PCR detection of the viral genome (vg) in pancreas, BAT, eWAT, subcutaneousWAT (scWAT), muscle and liver from *Cdk4^{fllox/fllox}* infected with systemic administration of AAV8-mini/aP2-null or AAV8-mini/aP2-cre (4×10^{12} vg) virus. Tissues were harvested 5 weeks post infection (n=5). (K) Relative mRNA levels of CDK4 in eWAT, scWAT, BAT and liver from *Cdk4^{fllox/fllox}* mice infected with AAV8-mini/aP2-null or AAV8-mini/aP2-cre virus were determined by RT-qPCR (n=5-4). (L) Percentage of lean mass of 14-16-week-old *Cdk4^{fllox/fllox}* infected with AAV8-mini/aP2-null or AAV8-mini/aP2-cre 3 weeks post infection (n= 5-4). (M) Percentage of lean mass of 30-week-old of *E2f1^{+/+}*, *Cdk4^{R24C/R24C} E2f1^{+/+}* and *Cdk4^{R24C/R24C} E2f1^{-/-}* mice (n= 4-6-12). (N) Western blot analysis showing Ki67 expression in eWAT from *E2f1^{+/+}*, *Cdk4^{R24C/R24C} E2f1^{+/+}* and *Cdk4^{R24C/R24C} E2f1^{-/-}* mice (n=4). (O) Hematoxylin and eosin staining of intestine, liver and lung sections from 31-34-week-old or 60-week-old *Cdk4^{+/+}* and *Cdk4^{R24C/R24C}* mice (n=5). (P) Body weight and percentage of fat and lean mass of *Cdk4^{+/+}* and *Cdk4^{R24C/R24C}* at age 31-34 weeks (n=8-8), age 51-54 weeks (n=12-12) and age 60 weeks (n=9-18). (Q) Protein expression of Cyclin D3 and actin in visceral adipose tissue samples from human subjects (R) Quantification of cyclin D3 expression in VAT from human subjects with BMI<27 and >27 (n=14-14). Data were expressed as mean \pm s.e.m. Significant differences were determined with unpaired 2-tailed Student's t-tests and are indicated by asterisks corresponding to *p<0.05.



G



H

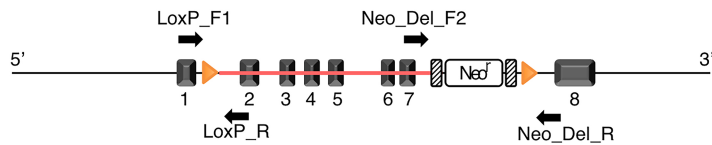
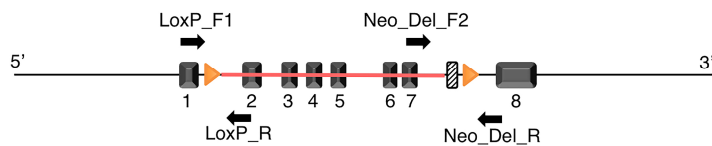
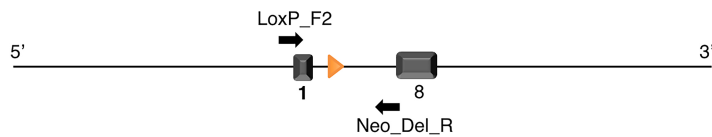


I

Wild type

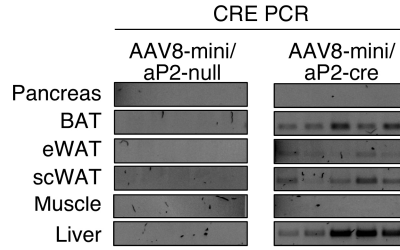


Targeting vector

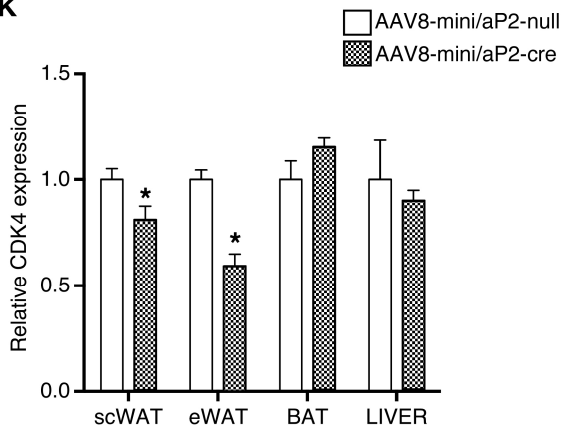
Conditional KO allele
(After Flp recombination)Constitutive KO allele
(After Cre recombination)

 LoxP site
  Frt site
  Exon
  Conditional KO region

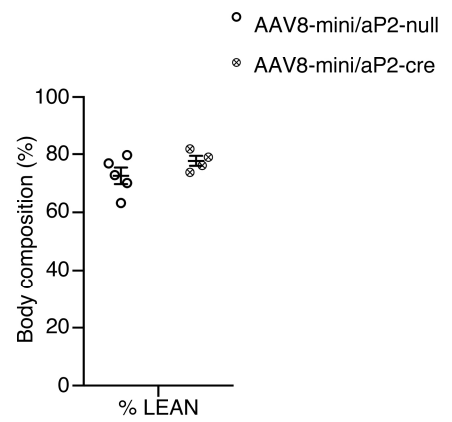
J



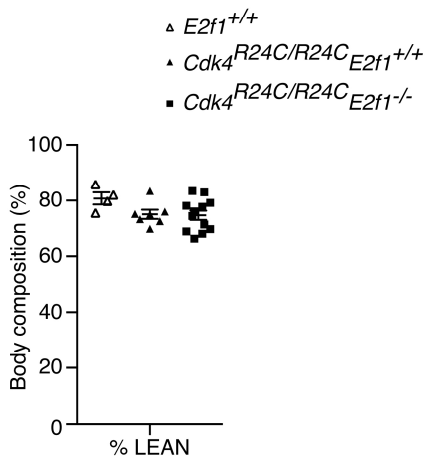
K



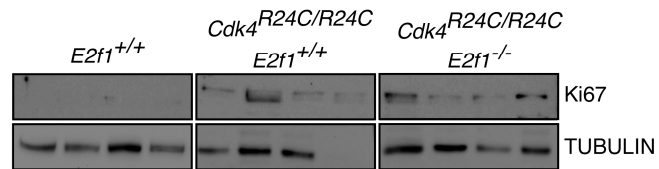
L



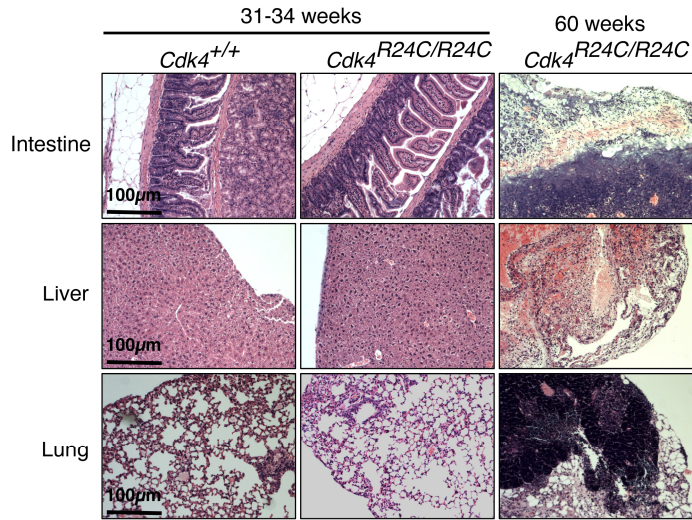
M



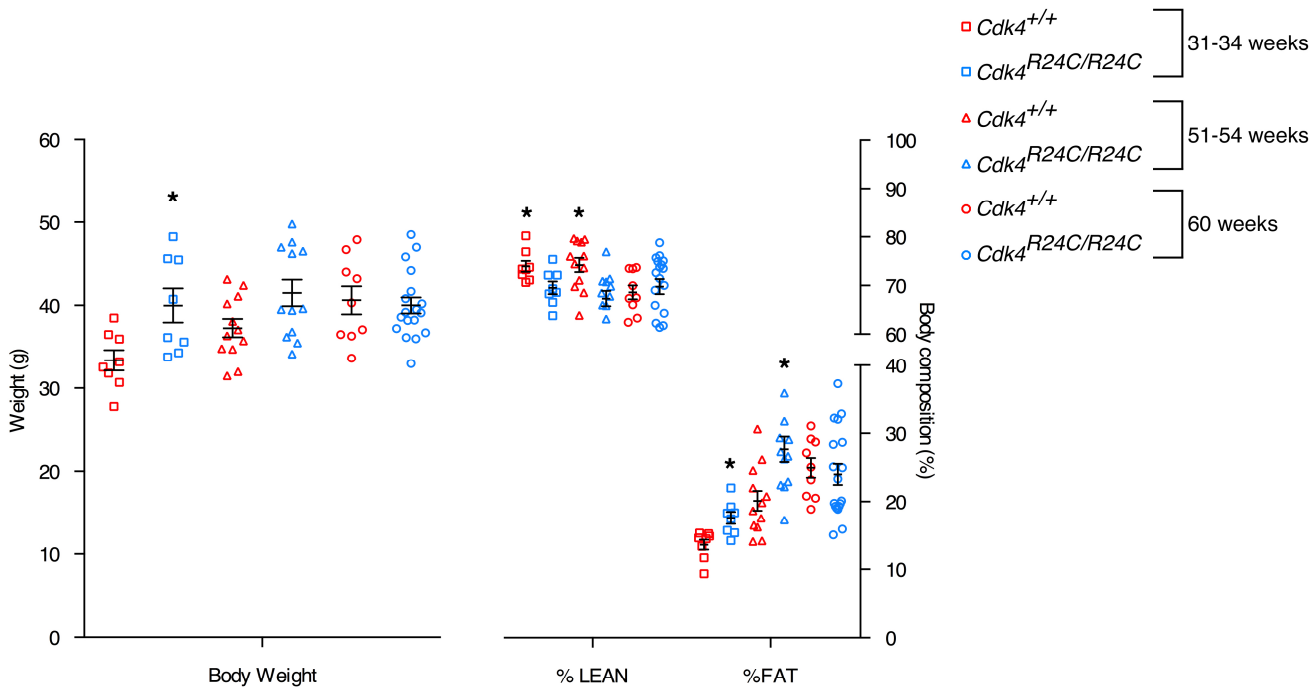
N



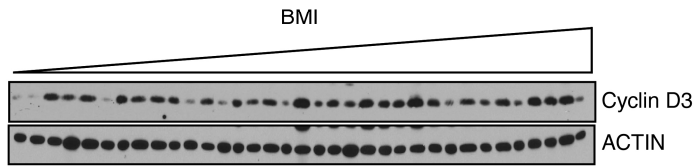
O



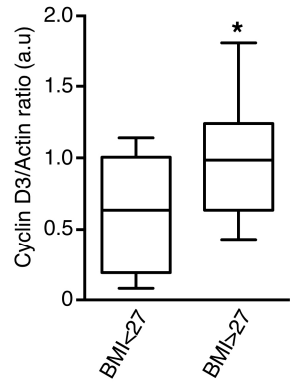
P



Q

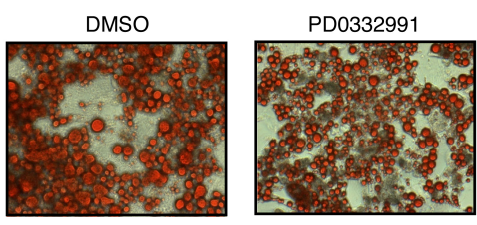


R

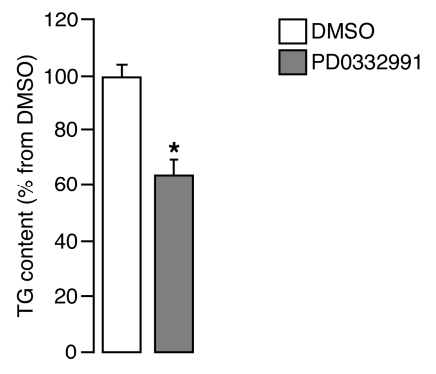


Supplemental Figure 2. (A) Oil red O staining of mature 3T3-L1 adipocytes treated with PD0332991 for 15 days (n=3). A representative image blot is shown. (B) TG quantification in 3T3-L1 mature adipocytes treated with a PD0332991 or with DMSO (n=3). (C) Rate of glycerol release in WAT explants from 23-week-old fasting *Cdk4^{+/+}* and *Cdk4^{nc}* mice (n=3). (D) Rate of NEFA release in WAT explants from fasting 28-week-old *Cdk4^{+/+}* and *Cdk4^{R24C/R24C}* of mice (n=6). (E-F) Liver TG content from 25-27-week-old *Cdk4^{+/+}* and *Cdk4^{nc}* mice (n=6-7) (E) and 33-40-week-old *Cdk4^{+/+}* and *Cdk4^{R24C/R24C}* mice (n=7-10) (F). Data were expressed as mean \pm s.e.m. Significant differences were determined with unpaired 2-tailed Student's t-tests and are indicated by asterisks corresponding to *p<0.05.

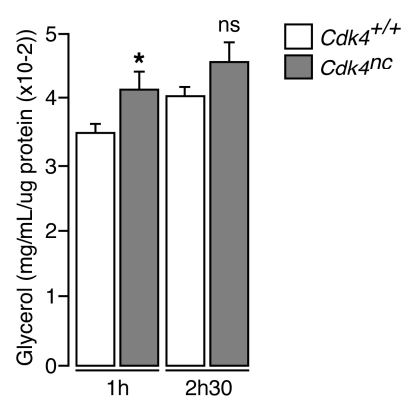
A



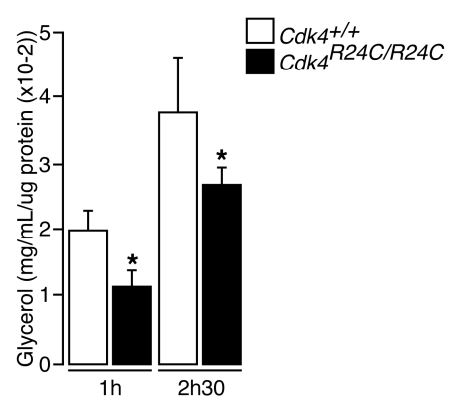
B



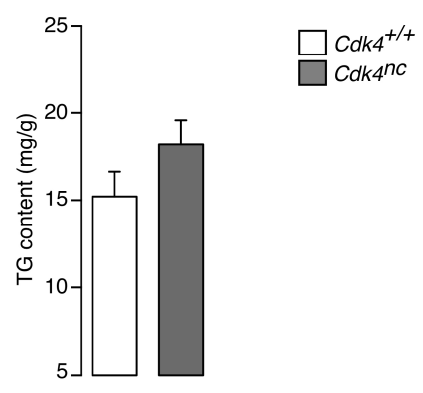
C



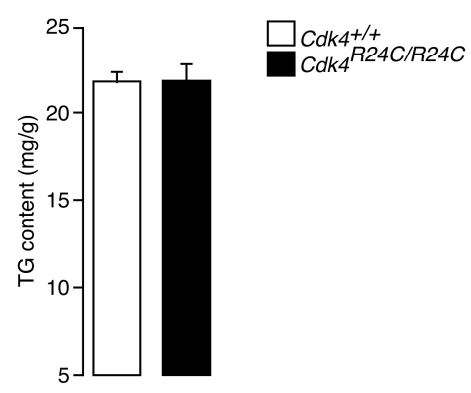
D



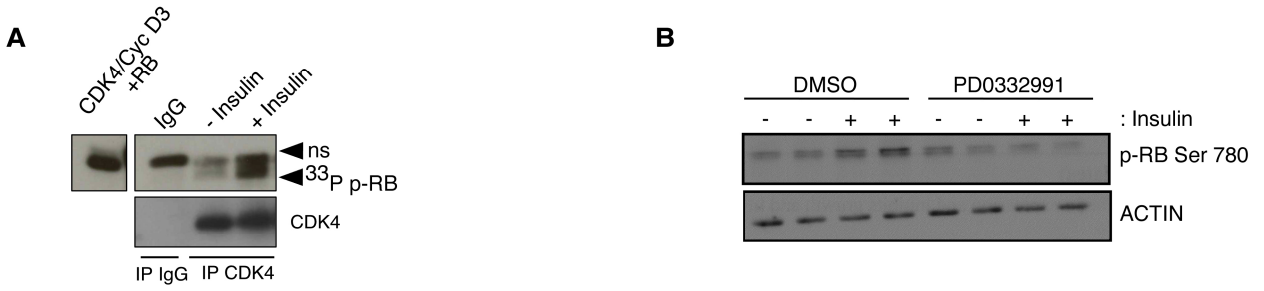
E



F



Supplemental Figure 3. (A) CDK4 activity *in vivo*. SDS-PAGE autoradiography showing pRB phosphorylation by CDK4. CDK4 was immunoprecipitated from WAT after insulin stimulation, and CDK4 activity was tested. The left panel shows RB phosphorylation by recombinant CDK4, it is used as a positive control of the experiment (B) Western blot analysis showing inhibition of insulin-induced pRB phosphorylation on Ser⁷⁸⁰ by PD03322991 treatment in mature 3T3-L1 adipocytes. (C) List of the peptides that are significantly ($p < 0.1$) differentially phosphorylated in serine/threonine kinase microarrays incubated with lysates from *Cdk4^{-/-}* versus the control mice treated with insulin for 3 min. Peptides with decreased phosphorylation when compared to *Cdk4^{+/+}* samples are labeled in blue; and peptides with increased phosphorylation when compared to *Cdk4^{+/+}* samples are labeled in red. (D) List of the peptides that are significantly ($p < 0.1$) differentially phosphorylated in serine/threonine kinase microarrays incubated with lysates from starved 3T3-L1 mature adipocytes treated with insulin in the presence of PD0332991. Peptides with decreased phosphorylation when compared to DMSO treated samples are labeled in blue, and peptides with increased phosphorylation when compared to DMSO treated samples are labeled in red. (E) Volcano plot showing differences in putative kinase activities between control and 3T3-L1 mature adipocytes treated with insulin in the presence of PD0332991. Kinases with a positive kinase statistic show higher activity in PD0332991 treated samples compared to control samples, whereas kinases with negative kinase statistic show lower activity in DMSO treated samples compared to control samples (F) List of the putative kinase substrate with the most significant differences in the activity between 3T3-L1 mature adipocytes treated with insulin in the presence of PD0332991 versus the DMSO condition. (G) Chemical CDK4 inhibition decreased insulin-stimulated AKT phosphorylation on Thr³⁰⁸ and Ser⁴⁷³. A-B and G panels are representative of least 3 independent experiments. A representative Western blot is shown.

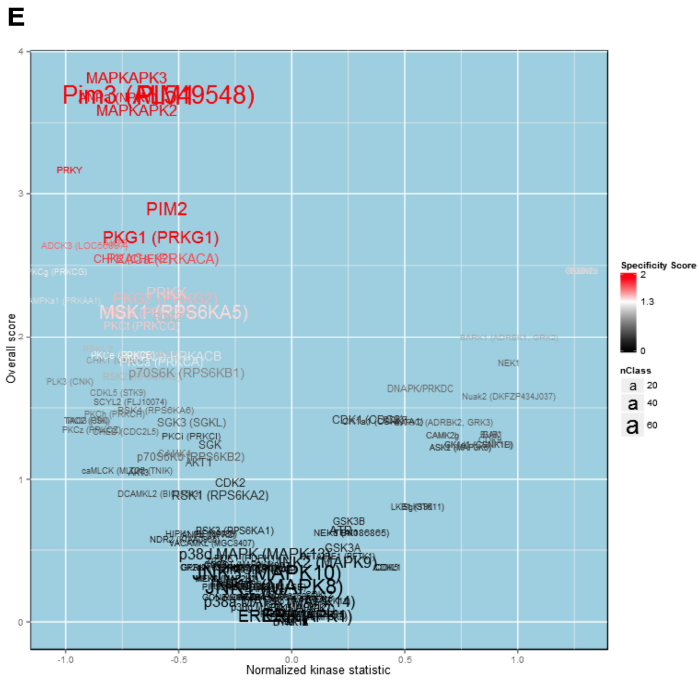


C

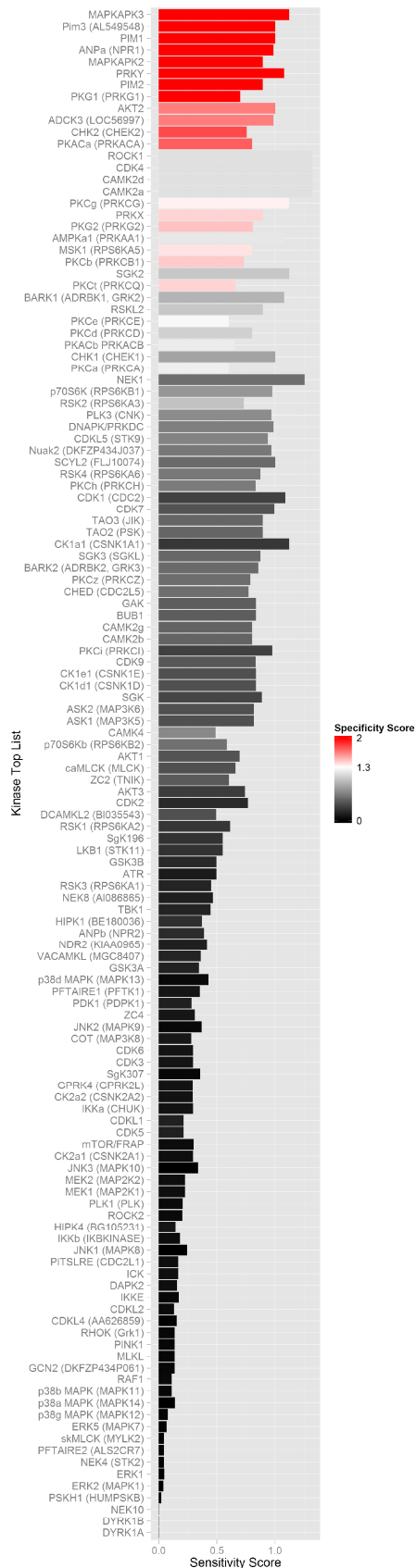
Peptide ID	UniprotAccession	Log fold change	P value
SRC_413_425	P12931	-6.32E-01	9.71E-03
CREB1_126_138	P16220	-6.44E-02	8.29E-02
MYPC3_268_280	Q14896	-5.10E-02	1.94E-02
ADRB2_338_350	P07550	-4.12E-02	1.58E-02
FRAP_2443_2455	P42345	-3.38E-02	1.64E-02
CFTR_730_742	P13569	-2.93E-02	1.80E-02
NR4A1_344_356	P22736	-1.88E-02	9.45E-03
KCNA2_442_454	P16389	-1.74E-02	6.87E-02
VTNC_390_402	P04004	-1.57E-02	3.25E-02
BAD_93_105	Q92934	-1.55E-02	6.59E-02
KAP3_107_119	P31323	-6.80E-03	6.27E-02
PTN12_32_44	Q05209	-3.65E-03	9.50E-02
K6PL_766_778	P17858	-4.20E-04	6.63E-02
CAC1C_1974_1986	Q13936	5.63E-03	8.59E-02
MARCS_152_164	P29966	6.82E-03	2.19E-02
MARCS_160_172	P29966	3.29E-02	4.07E-02
CD2_154_169	P06493	4.34E-02	6.33E-02

D

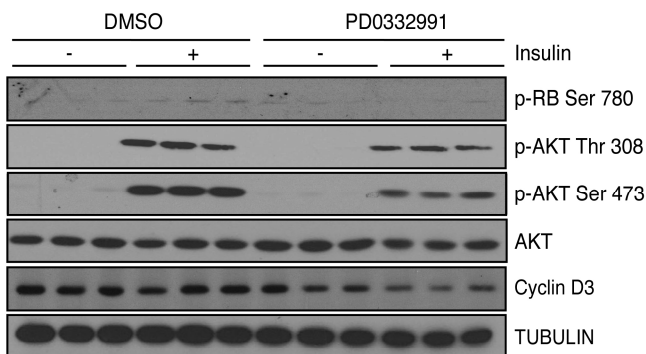
Peptide ID	UniprotAccession	Log fold change	P value
RADI_559_569	P35241	-1.81E+00	4.39E-02
KPCB_19_31_A25S	P05771	-1.13E+00	3.34E-02
KCNA3_461_473	P22001	-9.40E-01	7.66E-02
H2B1B_27_40	P33778	-8.97E-01	7.19E-02
GYS2_1_13	P54840	-8.44E-01	3.31E-02
KCNA1_438_450	Q09470	-8.21E-01	7.59E-02
ANXA1_209_221	P04063	-7.99E-01	6.75E-02
COF1_17_29	P23528	-7.49E-01	4.50E-02
BAD_112_124	Q92934	-7.41E-01	9.00E-02
RAP1B_172_184	P61224	-7.20E-01	8.58E-02
CENPA_1_14	P49450	-7.03E-01	6.61E-02
RAF1_253_265	P04049	-6.85E-01	7.77E-02
PLM_76_88	O00168	-6.08E-01	8.04E-02
PLEK_106_118	P08567	-5.54E-01	6.10E-02
PDE5A_95_107	O76074	-5.31E-01	2.08E-02
VASP_271_283	P50552	-5.27E-01	3.82E-02
E1A_ADE05_212_224	P03255	-4.87E-01	8.15E-02
NFKB1_330_342	P16898	-4.64E-01	7.80E-02
PPR1A_28_40	Q13522	-4.61E-01	4.61E-02
RYR1_4317_4329	P21817	-4.20E-01	9.87E-02
KPB1_1011_1023	P46200	-3.47E-01	5.20E-02
K6PL_766_778	P17858	-3.42E-01	4.16E-02
DESP_2842_2854	P15924	-3.32E-01	5.48E-02
CREB1_126_138	P16220	-3.26E-01	9.92E-02
BAD_93_105	Q92934	-2.72E-01	7.74E-02
KIF2C_105_118_S106G	Q99661	-2.65E-01	9.66E-02
EPB42_241_253	P16452	-2.60E-01	4.86E-02
ERBB2_679_691	P04626	-2.34E-01	7.90E-02
LMNB1_16_28	P20700	-2.07E-01	3.40E-02
BAD_69_81	Q92934	-1.95E-01	5.62E-02
AODB_706_718	P35612	-1.25E-01	5.71E-02
H32_3_18	Q71D13	-1.17E-01	6.04E-02
MIRIP1_172_184	P30304	-8.04E-02	2.38E-02
RB_803_815	P06400	-8.01E-02	1.72E-02
BCKD1_45_57	O14874	-7.39E-02	5.84E-02
KAPCG_192_206	P22612	-6.43E-02	9.93E-02
CDK7_163_175	P50613	-6.07E-02	3.12E-02
ERF_519_531	P50548	-5.88E-02	1.71E-02
KSSA1_374_386	Q15418	-5.47E-02	6.98E-02
ACM1_444_456	P11229	-3.34E-02	3.91E-02
DCX_49_61	O43602	-3.12E-02	1.99E-02
KPCB_626_639	P05771-2	-2.30E-02	5.70E-02
RDPK1_27_39	O15530	6.37E-02	2.22E-02
MPH6_140_152	Q99547	6.79E-02	7.95E-02
CDN1B_151_163	P46527	1.34E-01	6.02E-02
TAU_524_535	P10636	1.90E-01	8.99E-02
ATM_1972_1984	Q13315	2.15E-01	5.69E-02
MYBB_513_525	P10244	2.78E-01	6.21E-02
PRKDC_2618_2630	P78527	5.93E-01	1.69E-02
GSK21_355_367	P68400	7.36E-01	6.62E-02



F

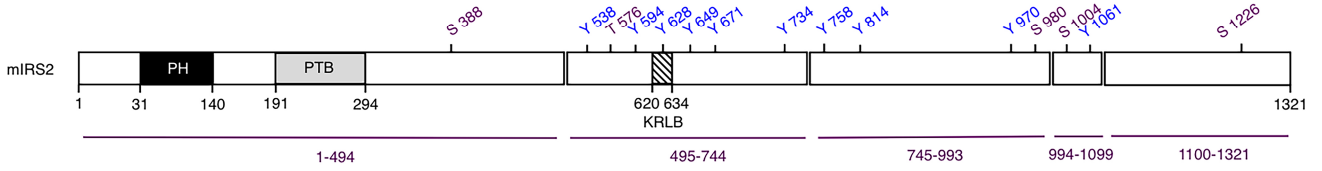


G



Supplemental Figure 4. (A) Schematic diagram of the truncated IRS2 protein fractions used to map the CDK4 sites. Subdomain organization and the localizations of tyrosine-phosphorylation sites and of CDK4 consensus sites are drawn to linear scale. Tyrosine-phosphorylation sites that are PI3K recruitment sites are labeled in blue. The CDK4 consensus sites for IRS2 are labeled in purple. (B) Alignment of IRS2 amino acid sequence through different species.

A

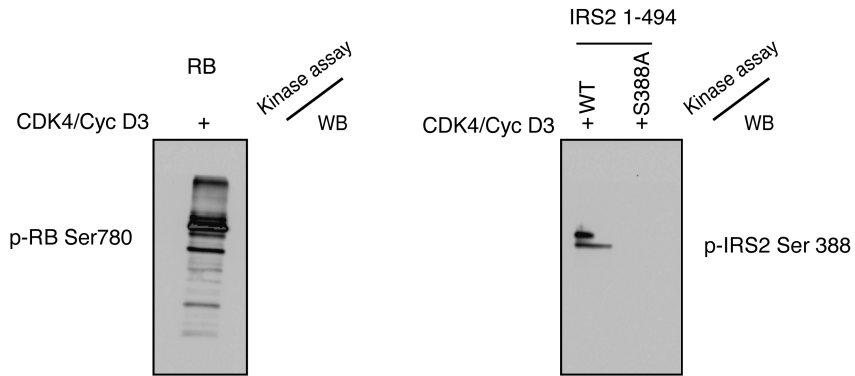
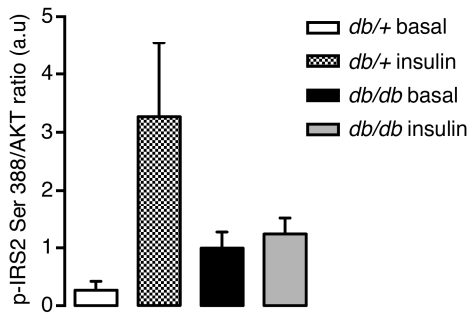
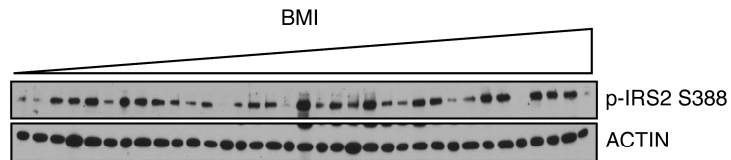
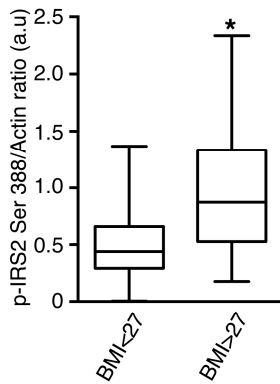
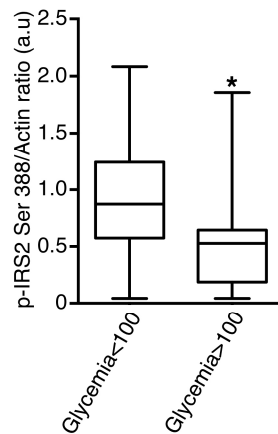


B

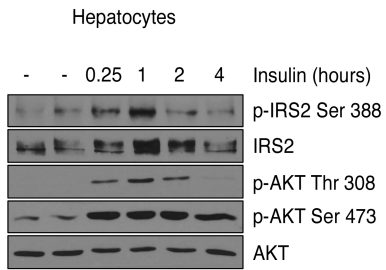
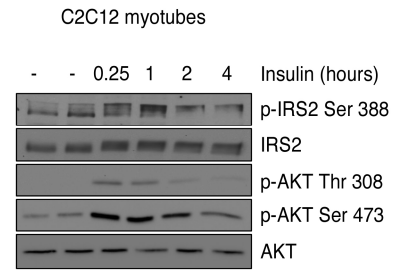
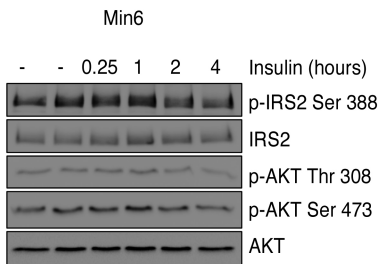
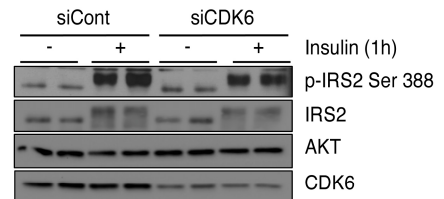
IRS2

	Mouse	382	VAGSPL SP GRVRAPLS	397
Site 1	Rat	383	VAGSPL SP GRVRAPLS	398
	Human	385	VAGSPL SP GRVRAPLS	400
	Mouse	1220	CPGGSS SP MRRETSVG	1235
Site 5	Rat	1223	CPGGSS SP MRRETSVG	1238
	Human	1231	CPGSGG SP MRRETSAG	1246

Supplemental Figure 5. (A) Validation of the generated IRS2 Ser³⁸⁸ specific antibody by a CDK4 *in vitro* kinase assay. The WT or S388A fragment GST-IRS2 1-494aa and recombinant RB were incubated in kinase conditions in the presence of the recombinant cyclin D3-CDK4. The SDS-PAGE gel was transferred to nitrocellulose and incubated with RB Ser⁷⁸⁰ antibody (left panel), and with the IRS2 Ser³⁸⁸ specific antibody (right panel) (n=1). (B) Quantification of IRS2 Ser³⁸⁸ phosphorylation of 9-11-week-old of *db/+* versus *db/db* mice in basal state and after treatment for 50 min with insulin (n=5). (C) The correlation between the pIRS2 Ser 388/actin ratio in visceral adipose tissue (VAT) and the BMI of the subjects is shown by a representative western blot. (D) Quantification of the pIRS2 Ser 388/actin ratio in VAT from human subjects with BMI <27 and >27 (n=14-31). (E) Quantification of the pIRS2 Ser³⁸⁸/actin ratio in VAT from human subjects with glycemia <100 and >100 (n=15-15). Data were expressed as mean \pm s.e.m. Statistically significant differences were determined with an unpaired 2-tailed Student's t-test and are indicated by asterisks corresponding to *p<0.05.

A**B****C****D****E**

Supplemental Figure 6. (A-C) Immunoblot analysis of IRS2 phosphorylation on Ser³⁸⁸ and AKT phosphorylation on Thr³⁰⁸ and Ser⁴⁷³ during a time course insulin stimulation in primary hepatocytes (A), C2C12 Myotubes (B) and Min 6 cells (C). (D) Immunoblot analysis of IRS2 phosphorylation on Ser³⁸⁸ in mature adipocytes transfected with siRNA against CDK6 and treated with insulin (n=2). Unless specified otherwise all experiments are the average of three independent experiments. A representative Western blot is shown.

A**B****C****D**

Supplemental Table 1. Primers used for qPCR and CRE PCR

Mouse mRNA primers :

Rs9	CGGCCCGGGAGCTGTTGACG CTGCTTGCGGACCCTAATGTGACG
Cdk4	AGCCGAGCGTAAGATCCCCT CAGCTGCTCCTCCATTAGGA

CRE PCR primers :

AAC ATG CTT CAT CGT CGG
TTC GGA TCA TCA GCT AA CC

SUPPLEMENTAL EXPERIMENTAL PROCEDURES

Subcellular Determination. Subcellular fractionation was performed using a commercial kit according to the manufacturer's instructions (NE-PER [78833] and Subcellular proteins fractionation kit [78840] from Thermo Scientific).

Triglyceride and insulin measures. Triglyceride (TG) content was assessed using a commercial kit according to the manufacturer's instructions (TG Diatools [Dia00660]), and values were normalized to protein content. Plasma concentration of insulin levels was determined using the insulin (Mouse) Ultrasensitive EIA (ALPCO Diagnostics).

Tissue digestion and cell fractionation. For tissue digestion, epididymal fat pads were isolated from mice, washed in phosphate-buffered saline (PBS), minced, and washed in Krebs-Ringer Bicarbonate HEPES (KRBH) buffer (pH 7.4). The tissues were incubated with collagenase type II (0.25 mg/ml) at 37°C for 20 min. Adipocytes were then separated from other cells with low-speed (200 × g) centrifugation. The medium below the adipocyte layer was centrifuged at 500 × g for 10 min to obtain the stromal vascular fraction.

Electroporation. *Irs2*^{-/-} pre-adipocytes were electroporated using the Neon transfection system (Invitrogen) according to manufacturer's recommendations. Briefly, 1 million cells were collected and resuspended in 10 µl Nucleofector solution. For overexpression in *Irs2*^{-/-} pre-adipocytes, 0.5 µg/µl of the corresponding plasmids were used. 12 hours after transfection, the cells were incubated overnight in serum-free DMEM containing 0.2% fatty acid-free BSA and stimulated with or without insulin (100 nM) for 20 min.

siRNA transfection of 3T3-L1 mature adipocyte. Transfection of 3T3-L1 was conducted with cells differentiated for 8 days and was performed as described previously (1). Cells were suspended by mild trypsinization and transfected using the Lipofectamine RNAiMAX Transfection reagent at 1.4µl/cm² (Life Technologies) according to manufacturer's recommendations. The plates were collagen-coated throughout these experiments. Small interfering RNA (siRNA), 35nM ON-TARGET SMARTpool siRNA CDK4 and 35nM ON-TARGET SMARTpool siRNA CONTROL (Thermo Scientific) or 75nM siRNA CDK6 (sc-35048) and 75nM siRNA CONTROL (sc-37007) (Santa cruz) were delivered into adipocytes. The adipocytes were replated and incubated at 37°C, 5%CO₂ for 24 hours before the media was exchanged for DMEM, 10% FBS.

RT-qPCR analysis. Tissue samples were snap-frozen in liquid nitrogen immediately after collection, grinded with liquid nitrogen using a mortar and a pestle, and dissolved in TRIreagent

(Sigma). RNA was obtained according the manufacturer's instruction. To eliminate residual viral genome (vg), total RNA was treated with Turbo DNase (Life Technologies). RNA was reverse transcribed using Super script II (Life Technologies). qPCR analysis was performed with a 7900HT instrument (Applied Biosystem) and SYBER Green detection of the amplified products. The relative quantification for a given gene was corrected to RS9 mRNA values. (Oligonucleotide sequences in Supplemental Table 1)

CRE PCR. Tissues were digested 30 min at 95°C in a lysis buffer containing 40 mM NaOH, 0.2 mM EDTA. An equal volume of buffer containing 40 mM Tris HCl (pH 5) was added to the samples to obtain DNA. PCR analysis of DNA samples was performed with primers specific for CRE detection. (Oligonucleotide sequences in Supplemental Table 1)

Administration of AAV8 vectors. AAV8-mini/aP2-null and AAV8-mini/aP2-cre virus were generated and produced as previously described (2). AAV8 vectors were injected by systemic administration (4×10^{12} viral genome) diluted in 200 μ L saline into the lateral tail vein.

Immunofluorescence, oil red O staining. For overexpression *Irs2*⁺ cells were washed with cold PBS and fixed with 4% paraformaldehyde and 4% sucrose for 15 min at RT. Cells were washed with PBS and permeabilized with 0.25% Triton X-100 for 5 min and blocked with 10% BSA in PBS for 45 min at 37°C. Cells were incubated with a combination of antibodies directed against Flag and pAKT Ser473 for 2 h at 37°C. Immunofluorescence labeling was revealed with Alexa-conjugated 594 anti-mouse and Alexa-conjugated 488 anti-rabbit secondary antibodies (Life Technologies) and Hoechst. Quantification of p-AKT Ser473 was performed with ImageJ software (National Institutes of Health) in 10 different areas of every cell to obtain a mean of signal per cell. Oil Red O staining was performed as described previously (3). Briefly, 3T3-L1 cells were fixed in 4% formaldehyde in PBS for 15 min at 4°C, and stained with Oil Red O for 20 min at RT. A stock solution of Oil Red O was prepared at 0.5% in isopropanol, and a working solution was prepared at a 3:2 ratio of Oil Red O/deionized water.

Histological analysis. eWAT, intestine, lung and liver samples were fixed in 4% paraformaldehyde (pH 7.4) overnight, embedded in paraffin, and serially sectioned at 4 μ M. Standard hematoxylin and eosin staining was performed on these sections.

Lipogenesis experiments. Lipogenesis experiments were performed with adipose tissue explants from fasted *Cdk4*^{+/+}, *Cdk4*^{nc}, and *Cdk4*^{R24C/R24C} mice incubated in DMEM containing 10% FBS. Explants were then labeled in triplicate with 1.0 μ Ci ¹⁴C acetate for 1 h or 2.5 h. Total lipids were extracted with 5 ml Folch mixture (chloroform:methanol, 2:1 [v/v]) and 500 μ l

water, and then dried under gaseous nitrogen. Labeled lipids were then subjected to thin-layer chromatography (TLC) in hexane:diethyl ether:acetic acid 90:10:1 (v/v) to separate triglycerides, diglycerides, and phospholipids. Air-dried plates were scanned on a PhosphorImager (GE Healthcare), and fatty acid spots on TLC were analyzed with the Typhoon 9200 PhosphorImager software (GE Healthcare). Values were normalized to protein contents, and areas are expressed as mean \pm s.e.m.

Lipolysis experiments. *Ex vivo* lipolysis experiments were performed with adipose tissue explants from fasted *Cdk4^{+/+}*, *Cdk4^{-/-}*, and *Cdk4^{R24C/R24C}* mice incubated in serum-free DMEM containing 3% fatty acid-free BSA. Conditioned medium was then analyzed for glycerol with the Free Glycerol Determination Kit (Sigma) and the NEFA kit (Wako Chemicals). Adipose tissue explants were then rinsed with PBS and harvested in lysis buffer. The protein contents of tissue lysates were determined with the Bradford Protein Assay (BioRad) and are expressed as mean \pm s.e.m.

Quantitative magnetic resonance. To measure total fat mass was in accurate manner, quantitative magnetic resonance (QMR) measurements were performed using the EchoMRI™ following the manufacturer instructions. Essentially, scans were completed placing animals in a plastic cylinder. Slight movements during the scanning process were acceptable. In the tube, animals were briefly subjected to a low-intensity electromagnetic field to detect and differentiate fat tissue from lean tissue.

Human samples and protein extraction.

We received human samples from two different institutions

- Human adipose tissue samples were obtained from an adipose tissue biobank collection at the Joan XXIII University Hospital from Tarragona, Spain. Appropriate Institutional Ethics Committee approval written informed concern was obtained from all participants. Visceral adipose tissue samples were obtained during cholecystectomy or surgery for abdominal hernia during a scheduled surgical procedure. All the patients had fasted overnight for at least 12 h before the surgical procedure. Samples were collected and washed in 1 \times PBS, immediately frozen in liquid nitrogen, and stored at -80°C. All the subjects were of Caucasian origin and reported that their body weight had been stable for at least 3 months before the study. They had been free of any infections during the month before the study. Primary cardiovascular disease, arthritis, acute inflammatory disease, and renal diseases were specifically excluded by biochemical work-ups. Patients on lipid-lowering drugs were excluded.

- All of the participants gave their written informed consent, and the study was reviewed and approved by the Ethics and Research Committee of Virgen de la Victoria Clinical University Hospital, Malaga, Spain. All obese patients underwent biliopancreatic diversion of Scopinaro. Morbidly obese patients were excluded if they were receiving insulin or hypoglycemic agents, had cardiovascular disease, arthritis, acute inflammatory disease, infectious disease, or were receiving drugs that could alter the lipid profile or the metabolic parameters at the time of inclusion in the study. The nonobese patients were selected from among patients who underwent laparoscopic surgery for hiatus hernia or cholelithiasis with no alterations in lipid or glucose metabolism, with a similar age, and with the same selection criteria as those for the morbidly obese group. All of the patients were of Caucasian origin.

Samples were stored at -80°C , reduced into powder form with liquid nitrogen using a mortar and a pestle. Protein extractions were carried out using the M-PER mammalian extraction buffer (Thermo Scientific) containing 1:50 Halt phosphatase inhibitor cocktail (Thermo Scientific) and 1:50 Halt protease inhibitor cocktail EDTA-free (Thermo Scientific) for 30 minutes at 4°C . The lysates were then centrifuged twice at 13.000 r.p.m. for 20 min to remove all debris and fat. Protein samples were stores at -80°C .

Statistics. Data are expressed as mean \pm s.e.m. Statistically significant differences were determined with unpaired 2-tailed Student's t-tests and are indicated by asterisks corresponding to $*p<0.05$.

SUPPLEMENTAL REFERENCES

1. Kilroy, G., Burk, D.H., and Floyd, Z.E. 2009. High efficiency lipid-based siRNA transfection of adipocytes in suspension. *PLoS One* 4:e6940.
2. Jimenez, V., Munoz, S., Casana, E., Mallol, C., Elias, I., Jambrina, C., Ribera, A., Ferre, T., Franckhauser, S., and Bosch, F. 2013. In vivo adeno-associated viral vector-mediated genetic engineering of white and brown adipose tissue in adult mice. *Diabetes* 62:4012-4022.
3. Iankova, I., Chavey, C., Clape, C., Colomer, C., Guerineau, N.C., Grillet, N., Brunet, J.F., Annicotte, J.S., and Fajas, L. 2008. Regulator of G protein signaling-4 controls fatty acid and glucose homeostasis. *Endocrinology* 149:5706-5712.